though the highest peaks of the Southern Alps occur southeast of Franz Josef, where after 140×10^3 years ago uplift is inferred to be maximum, the area of highest metamorphic grade of schist and hence expected maximum total uplift occurs 25 to 40 km northeast of the Haast River.

The close altitudinal spacing of marine terraces along the coast west of the Alpine fault between the Stafford Range and the Moeraki River suggests relatively low uplift rates, so we surveyed altitudes of uplifted shore platforms in conjunction with topographic map analyses. Attempts to correlate six marine terraces in the coastal mountains with New Guinea terraces yielded only one reasonable solution (Fig. 3). Uniform inferred uplift of 2.0 m per 10^3 years between 242×10^3 and 176×10^3 years ago decreased to uniform uplift of 0.87 m per 10^3 years since roughly 150×10^3 years ago.

Correlations of remnants of marine terraces along the northwestern flank of the Southern Alps at three widely spaced sites with the dated sequence of global marine terraces at New Guinea is a useful basis for inferring terrace ages and uplift rates. At least 250 km of the Southern Alps is being elevated at an inferred rate of 5 to 8 m per 10^3 years during the last 135×10^3 to 140×10^3 years. Reset K/Ar radiometric clocks in heated and uplifted schist, and surficial temperature gradients, imply uplift rates of less than 10 m per 10^3 years (*11*); these cross-checks agree with the uplift rates inferred from the marine-terrace analyses. An apparent doubling of uplift rate occurred between 135×10^3 years and 140×10^3 years ago at three widely separated sites east of the Alpine fault. Presumably, it is associated with long-term increasing convergence between the Australian and Pacific plates. Opposite and roughly synchronous changes in inferred uplift rates east and west of the Alpine fault near the Haast River also contribute to the picture of internal consistency that supports the correlations and uniform uplift-rate assumption.

REFERENCES AND NOTES

1. F. J. Vine and D. H. Matthews, *Nature (London)* **199**, 947 (1963); J. Heirtzler *et al.*, *J. Geophys. Res.* **73**, 2119 (1968).
2. W. B. Bull, in *Proceedings of the 15th Annual Binghamton Geomorphology Symposium*, M. Morisawa and J. T. Hack, Eds. (Allen and Unwin, Hemel Hempstead, United Kingdom, 1985), p. 129–152.
3. A. L. Bloom, W. S. Broecker, J. M. A. Chappell, R. K. Matthews, K. J. Mesolella, *Quat. Res. (N.Y.)* **4**, 185 (1974); J. M. A. Chappell, *Geol. Soc. Am. Bull.* **85**, 553 (1974); *Search* **14**, 99 (1983); written communication, 13 January 1983.
4. R. J. Walcott, *Bull. R. Soc. N.Z.* **18**, 4 (1979); J. Adams, *Geol. Soc. Am. Bull.* **91**, 1 (1980).
5. J. Adams, *Bull. R. Soc. N.Z.* **18**, 47 (1979).
6. A. F. Cooper and D. G. Bishop, *ibid.*, p. 35; G. J. van der Lingen, *ibid.*, p. 45.
7. A. G. Griffiths and M. J. McSaveny, *N.Z. J. Sci.* **26**, 293 (1983); M. R. Hawkes, thesis, University of Canterbury, Christchurch, New Zealand (1981).
8. R. M. Kirk, *N.Z. J. Geol. Geophys.* **20**, 571 (1977); W. C. Bradley and G. B. Griggs, *Geol. Soc. Am. Bull.* **87**, 433 (1976).
9. F. W. Taylor, C. Jouannic, A. L. Bloom, *J. Geol.* **93**, 419 (1985); R. K. Matthews, *Quat. Res. (N.Y.)* **3**, 147 (1973); R. E. Dodge, R.G. Fairbanks, L. K. Benninger, F. Maurrasse, *Science* **219**, 1423 (1983); P. J. Hearty, G. H. Miller, C. E. Stearns, B. J. Szabo, *Geol. Soc. Am. Bull.* **97**, 850 (1986); T. L. Ku, M. A. Kimmel, W. H . Easton, T. J. O'Neil, *Science* **183**, 959 (1974); T. Yoshikawa, Y. Ota, N. Yonekura, A. Okada, N. Iso, *Geog. Rev. Jpn.* **53**, 238 (1980); T. Yoshikawa, S. Kaizuka, Y. Ota, *The Landforms of Japan* (Univ. of Tokyo Press, Tokyo, 1981); T. L. Ku and J. P. Kern, *Geol. Soc. Am. Bull.* **85**, 1713 (1974).
10. Best age control is 133×10^3 years and younger ($\pm 3 \times 10^3$ years to 5×10^3 years), poorest is older than 214×10^3 years ($\pm 10 \times 10^3$ years to 15×10^3 years). Altitudes formed are ± 5 m, mean altitudes ± 15 m, and inferred uplift ± 20 m.
11. R. G. Allis, *Geology* **9**, 303 (1981); *International Symposium on Recent Crustal Movements Abstracts* (Royal Society of New Zealand, Wellington, 1984), p. 1.

12. We appreciate discussions with K. R. Berryman, A. L. Bloom, J. Bradshaw, J. Campbell, J. M. A. Chappell, B. Harrison, R. M. Kirk, P. L. K. Knuepfer, K. R. Lajoie, Y. Ota, R. P. Suggate, and H. W. Wellman. Supported by National Science Foundation grants EAR-815836 and EAR-8305892, U.S. Geological Survey contract 14-08-0001-21882, and the Otago University Research Grants Committee.

17 April 1986; accepted 19 August 1986

Polymorphism of Sickle Cell Hemoglobin Aggregates: Structural Basis for Limited Radial Growth

LEE MAKOWSKI AND BEATRICE MAGDOFF-FAIRCHILD

Fibers composed of molecules of deoxygenated sickle cell hemoglobin are the basic cause of pathology in sickle cell disease. The hemoglobin molecules in these fibers are arranged in double strands that twist around one another with a long axial repeat. These fibrous aggregates exhibit a pattern of polymorphism in which the ratio of their helical pitch to their radius is approximately constant. The observed ratio agrees with an estimate of its value calculated from the geometric properties of helical assemblies and the degree of distortion that a protein-protein interface can undergo. This agreement indicates that the radius of an aggregate is limited by the maximum possible stretching of double strands. The geometric properties limiting the radial extent of sickle hemoglobin fibers are fundamental to all cables of protein filaments and could contribute to the control of diameter in other biological fibers such as collagen or fibrin.

SICKLE CELL HEMOGLOBIN DIFFERS from normal hemoglobin only in that a valyl residue is substituted for a glutamate at the β6 position of both β chains of the molecule. In its unliganded state, the sickle cell hemoglobin (HbS) molecule has a lower solubility than normal hemoglobin. This results in an aggregation of the molecules into regular fibrous arrays. Much of the pathophysiology of sickle cell disease is attributed to occlusion of the capillaries in the microcirculation by fiber-containing erythrocytes. Observed polymorphic assemblies in vitro range in size from 220 Å diameter fibers (*1*) to larger macrofibers (*2, 3*), twisted crystals (*4*), and macroscopic crystals suitable for high-resolution x-ray crystallography (*5–7*). The crystals and the fibers found in erythrocytes and in solutions of deoxy-HbS have a common basic structural element, the presence of which has been confirmed by the striking similarities of their x-ray diffraction patterns (*8, 9*). This basic structural unit or protofilament is a double strand of HbS molecules, which possesses approximate twofold screw symmetry with an axial rise of 32 Å per hemoglobin molecule. The protofilament is stabilized, in part, by the interaction of one of the β6 residues in HbS with the edge of the heme pocket of an adjacent molecule (*7, 10*).

All of the aggregates of HbS molecules are side-to-side assemblies of the protofilaments. In the macroscopic crystals, the protofilaments are arranged parallel or antiparallel to one another. In the smaller aggregates, the protofilaments are slightly twisted, and coil around one another with a long helical pitch. From the side-to-side packing of protofilaments in the fibrous aggregates, it would appear possible to continue adding protofilaments to these aggregates without bound. The side-to-side packing of protofilaments is not self-limiting as it is, for instance, in the case of microtubules, where

L. Makowski, Department of Biochemistry and Molecular Biophysics, Columbia University, College of Physicians and Surgeons, 630 West 168 Street, New York, NY 10032.

B. Magdoff-Fairchild, Department of Medicine, Columbia University, College of Physicians and Surgeons, and Hematology Division, Medical Service St. Luke's–Roosevelt Hospital Center, New York, NY 10025.

the completion of a cylindrical shell precludes the further addition of protofilaments to the structure. Nevertheless, under well-defined conditions, fibers of relatively uniform size are observed, indicating that the growth of HbS fibers is self-limiting. The question being addressed in this report is: What are the physical and geometric factors determining the radial extent of HbS fibers?

Let us consider the general case. In a cable of identical periodic protofilaments, the subunits interact with one another to make specific bonds over the entire length of the protofilaments. If each protofilament has an intrinsic twist the protofilaments will wrap around one another in order to maintain a pattern of specific interactions over an extended axial distance. An example of this kind of structure is the two-stranded α-helical coiled-coil (*11*). A cable of two or more twisted protofilaments will itself be twisted, and its pitch will be the same as that of the individual protofilaments (*12*). In a twisted aggregate, the path length of the protofilaments on the surface will be greater than for those in the middle. For the protofilaments to maintain regular interactions with each other, those at large radius must necessarily be stretched relative to those at small radius (*13*). A model demonstrating the relation between the twist of a cable with regularly arrayed interactions and its constituent protofilaments is shown in Fig. 1. At any axial position in the cable, the cross-sectional arrangement of protofilaments is the same, but the entire arrangement rotates with axial progression along the length of the cable.

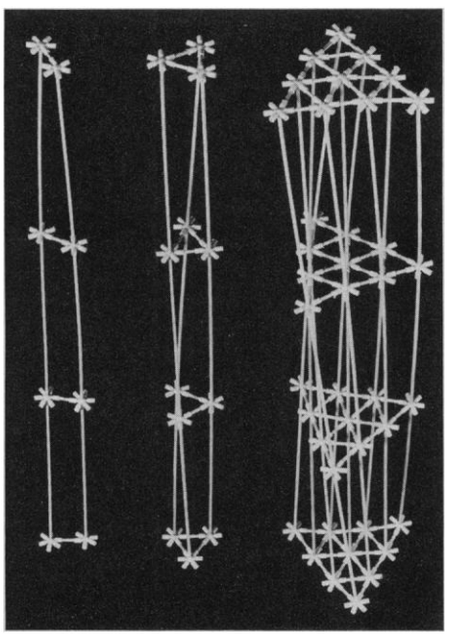

Fig. 1. Models of cables of twisted protofilaments. Each protofilament was constructed to have a 90° rotation along its length. Interaction of two protofilaments with one another (left) results in an aggregate having the same degree of twist as its constituent protofilaments, that is, about 90°. Addition of a third protofilament (center) increases the radius of each protofilament slightly but results in an aggregate in which the protofilaments are still not substantially distorted. In a larger aggregate (right) with ten protofilaments, the outer protofilaments are distorted in order to trace a helical path about the center of the aggregate. At a radius where the energy required to distort the protofilaments becomes greater than the energy of binding of the protofilaments, the aggregate will cease to grow. In addition to the distortion of the protofilaments at high radius, the rigidity of the protofilaments in these models has resulted in two additional distortions to the entire aggregate: the aggregate rotates by only about 60° along its length, meaning that each protofilament has been untwisted by about 30°. Furthermore, a slight bulging of the top surface can be observed in the photograph. The protofilaments near the center of the cable are being compressed while the ones at the outside are being stretched. This compression, if it occurs in protein assemblies, will lead to overestimates in the elongation calculated as described in the text.

As the radius of a cable increases, the path length of the protofilaments at the outer surface of the cable increases. The length, l, traced by a protofilament at a radius, r, necessary to span an axial distance equal to the pitch, p, is equal to

$$l = [p^2 + (2\pi r)^2]^{1/2} \quad (1)$$

Regular interactions between protofilaments within a cable can be maintained for a protofilament at a radius, r, only if the protofilament is stretched by an amount equal to the path length increase $(l - p)$. This is a necessary condition for maintenance of the regular interactions that stabilize a twisted aggregate.

The elongation within an aggregate, $e = l_{max}/p$, where l_{max} is the maximum protofilament length, will be small if the energy of interaction between protofilaments is small or if the protofilaments are relatively rigid. At the outer surface of the cable,

$$p/r = 2\pi/(e^2-1)^{1/2} \quad (2)$$

The pitch, radius, and elongation may change under different environmental conditions. A plot of pitch versus radius could be useful for distinguishing among several simple models of twisted aggregates whose structures depend on the effect of environmental conditions. Let us consider the following models:

1) Interactions within individual protofilaments remain unchanged, but the energy of interactions among protofilaments is altered by environmental changes. In such a case, the pitch of individual protofilaments will remain fixed and consequently the pitch of the aggregates will also remain fixed. If the energy of interactions among protofilaments is weakened by some environmental change (for example, an increase in ionic strength), then the elongation and the radius will both decrease. If they change according to Eq. 2 then a plot of pitch versus radius for this family of aggregates will result in a straight horizontal line.

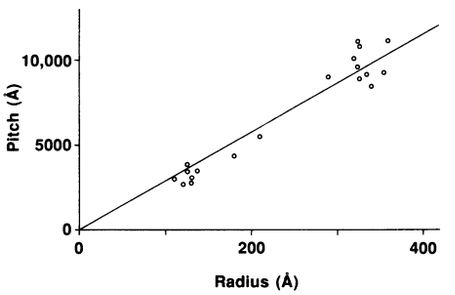

Fig. 2. A plot of radius versus pitch for the aggregates listed in Table 1, except the values for the twisted crystal (*15*). The slope of the least-squares line constrained to go through the origin for all aggregates is 27.75 (as plotted); for macrofibers alone, the slope is 29.6 and for fibers, 25.7. These numbers correspond to average changes in the center-to-center distances of 1.6 Å between axially interacting molecules (1.4 Å in the macrofibers and 1.9 Å in the fibers). Within 90% confidence limits, the average slope for macrofibers is in the range of 27.9 to 31.3, and for fibers it is in the range of 22.4 to 29.0. A shift of 1.5 Å per molecule corresponds to a slope of 28.9.

2) The pitch of an aggregate changes, while the energy of interaction among subunits within a protofilament and among different protofilaments (binding energy) both remain constant. In this case, the elongation remains constant but the pitch and radius may change according to Eq. 2. A plot of pitch versus radius for this family of aggregates would result in a straight line going through the origin with a slope of $2\pi/(e^2-1)^{1/2}$. More complex models could be formulated but it would be more difficult to distinguish among them with plots of pitch versus radius alone (*14*).

The derived relation of pitch to radius can be applied to fibers of deoxy-HbS. Twisted aggregates of HbS have been observed with pitch ranging from 3,000 to 80,000 Å. Table 1 lists the approximate pitch and radius of a variety of HbS aggregates as measured from published micrographs, and the elongation for each of these aggregates as calculated from Eq. 2. The aggregates, all of which consist of double strands of HbS molecules, fall into three categories: the fibers, which appear to be a relatively homogeneous population, and the macrofibers and twisted crystals that occur with different numbers of protofilaments. Relatively large variations of pitch have been observed among similar macrofibers or even within the same macrofiber (*3*).

The data in Fig. 2, which exclude the values for the twisted crystals (*15*), indicate

that the *p/r* ratio is similar for all of these aggregates. These data are consistent with a model where the effect of environmentally induced changes in HbS aggregates are similar to model (2) above. That is, the pitch of the protofilaments is changed but the energy of interactions among subunits does not change detectably.

The least-squares fit to the data constrained to go through the origin (Fig. 2) indicates a *p/r* ratio of 27.75, and suggests that the elongation is essentially the same for fibers and macrofibers. If the fit is not constrained to go through the origin, the *p/r* ratio is 32.44 and the intercept on the horizontal axis is at a radius of 28 Å ± 10 Å. Given that HbS molecules that interact with one another in a protofilament are displaced axially from one another by 32 Å (lateral interactions) and by 64 Å (axial interactions), these ratios correspond to an increase of 0.6 to 0.8 Å in the distance between HbS molecules interacting laterally, and 1.2 to 1.6 Å between molecules interacting axially.

Small relative shifts of adjacent structural elements have been observed in comparisons of insulin molecules in different crystal packing environments (*16*). Intramolecular helix-helix interactions remain unchanged when shifts are smaller than 1.5 Å. These small shifts can be taken up by rotations of side chains. If the shifts are greater than 1.5 Å, the interfaces must be restructured by breaking and then reforming of the bonds that participate in these interactions. Although these observations involve intramolecular shifts, detailed studies of protein-protein interactions indicate that intermolecular interactions among protein molecules are of the same nature as interactions between structural elements within a single protein molecule (*17*).

The magnitude of the elongation as calculated from the slope of the line in Fig. 2 suggests that the entire stretching of the protofilament can be accounted for by small changes in side-chain torsion angles at the intermolecular interfaces. The most highly stretched protofilaments on the outside of the fiber can accommodate the same set of intermolecular interactions that are present in the most highly compressed protofilaments at the smallest radius of the fiber. The fact that the plastic limit of interactions among secondary structures (*16*) is so close to the maximum degree of stretch observed in HbS aggregates suggests that this determines the limit for the stretching of HbS protofilaments. Put another way, the results reported here imply that the bonding energy generated by the side-to-side interactions of protofilaments is sufficient to distort and rotate bonds between secondary structures in a protofilament, but is not great enough to break any bonds and restructure the interfaces.

The picture of HbS aggregates emerging from this analysis is one in which double strands of relatively fixed pitch (under any given conditions) interact side-to-side to form aggregates with pitch equal to that of the individual protofilaments. In most cases, the pitch observed in any given environment is highly variable and may even be different for different turns of the same aggregate. Measurement errors, and the fact that the aggregates have all been imaged lying on an electron microscope grid immersed in negative stain will account for some of the variability. But changes in pitch may occur in any case since only minute changes in the intermolecular interactions would result in changes in pitch. For instance, the range of pitch observed for macrofibers with radii over 330 Å is 8,445 to 11,360 Å (Table 1). This difference can be accommodated by changes in the relative positions of side chains involved in axial interactions of less than 0.5 Å at the outside. Most groups involved in stabilizing the protofilament would move less than half that amount. Consequently, very little energy would be required to produce the large observed variations in pitch.

Our conclusion is that all of the intermolecular interactions stabilizing a protofilament are preserved during the stretching of the protofilament at the outside of an aggregate and the compression of the protofilament at the center of an aggregate. The interactions among HbS molecules in protofilaments at the surface of a fiber are quasi-equivalent (*18*) to the corresponding interactions in protofilaments at the center of a fiber. The radius of an aggregate is limited by the limited flexibility of intermolecular interactions and by the energy available for the stretching of a protofilament at the outer surface. This energy is generated by the bonds between the added protofilament and the aggregate. An aggregate will stop growing radially when the energy necessary for stretching a protofilament being added is greater than the energy generated by the binding of this protofilament to the aggregate. Consequently, assemblies of twisted protofilaments cannot be extended radially without bound.

A variety of other biological fibers, including collagen and fibrin, appear to be organized into twisted cables. Some regularity in the fiber diameter is observed in both of these systems. It seems likely that the geometric and energetic considerations outlined here will be important in understanding the control of fiber diameter in these and other biological systems.

Table 1. Radius and pitch of sickle cell hemoglobin aggregates. All dimensions are as measured from published electron micrographs except pitch and radius, quoted in (*19*). Sealy-S and J-Oxford-S are aggregates composed of hemoglobin containing HbS β chains and α chains having the designated mutation.

Pitch (Å)	Radius (Å)	*p/r*	*e*	Reference
		Macrofiber		
9,590	323	29.7	1.022	(*2*)
5,460	210	26.0	1.028	(*20*)
9,040	290	31.1	1.020	(*20*)
8,445	340	24.8	1.031	(*20*)
9,110	334	25.7	1.029	(*20*)
9,315	355	27.9	1.025	(*20*)
10,880	326	33.4	1.017	(*3*)
11,180	325	34.3	1.017	(*3*)
11,360	360	31.4	1.020	(*3*)
8,910	325	27.3	1.026	(*3*)
11,000	320	33.7	1.017	(*3*)
		Fibers		
3,000	110	27.3	1.026	(*21*)
2,664	130	20.5	1.046	(*21*)
3,902	124	31.2	1.020	(*1*)
3,463	136	25.4	1.030	(*21*)
3,510	125	28.1	1.025	(*21*)
2,600	120	21.7	1.041	(*21*)
		Sealy-S mutant		
4,300	180	23.9	1.034	(*19*)
		J-Oxford-S mutant		
3,100	130	23.8	1.034	(*19*)
		Twisted crystals		
80,770	1,270	63.6	1.005	(*4*)
80,745	1,040	77.6	1.003	(*4*)
83,000	1,500	55.3	1.006	(*4*)

REFERENCES AND NOTES

1. G. Dykes, R. H. Crepeau, S. J. Edelstein, *Nature (London)* **272**, 506 (1978).
2. M. J. Potel, T. E. Wellems, R. J. Vassar, B. Deer, R. Josephs, *J. Mol. Biol.* **177**, 819 (1984).
3. T. E. Wellems, R. J. Vassar, R. Josephs, *ibid.* **153**, 1011 (1981).
4. T. E. Wellems and R. Josephs, *ibid.* **137**, 443 (1980).
5. B. C. Wishner, K. B. Ward, E. E. Lattman, W. E. Love, *ibid.* **98**, 179 (1975).
6. E. A. Padlan and W. E. Love, *J. Biol. Chem.* **260**, 8272 (1985).
7. ———, *ibid.*, p. 8280.
8. B. Magdoff-Fairchild and C. C. Chiu, *Proc. Natl. Acad. Sci. U.S.A.* **76**, 223 (1979).
9. C. C. Chiu and B. Magdoff-Fairchild, *J. Mol. Biol.* **136**, 455 (1980).
10. R. Dickerson and I. Geis, *Hemoglobin: Structure, Function, Evolution and Pathology* (Benjamin/Cummings, Menlo Park, CA, 1983).
11. F. H. C. Crick, *Acta Crystallogr.* **6**, 689 (1953).
12. The pitch of a helical assembly of subunits is not uniquely defined. Any number of helical paths can be drawn through subsets of the subunits in a helical array. A one-start helix is defined as a helix that goes through all the subunits in a helical array. A two-start helix goes through half of the subunits. For an α-helix, the main chain follows a one-start helix with a pitch of about 1.5 Å. α-Helices involved in the coiled-coil interaction as described by Crick (*11*) interact along seven-start helices which wind about an ideal α-helix with a pitch of 189 Å. An "ideal" α-helical coiled-coil would then be expected to have a pitch of 189 Å. However, small changes in the twist per residue could cause relatively large changes in this pitch. In the HbS double strand the one-start helix has a pitch of about 64 Å. The two-start helices have the very long pitch corresponding to that of the fibrous aggregates. In this report, whenever we refer to the pitch of an HbS double strand we mean the pitch of the two-start helices.
13. Several authors have suggested that the limited radius of the HbS aggregates may be associated with

the twisting of the protofilaments: R. H. Crepeau *et al.*, *Proc. Natl. Acad. Sci. U.S.A.* **78**, 1406 (1981); S. J. Edelstein, *J. Mol. Biol.* **150**, 557 (1981); E. A. Padlan and W. E. Love, *J. Biol. Chem.* **260**, 8280 (1985).
14. These models assume that the only distortion that occurs on binding of a protofilament to an aggregate occurs within the protofilament being bound. In fact, whenever a protofilament is stretched on binding to an aggregate, the aggregate will exhibit a slight compression and untwisting (see Fig. 1). These distortions are distributed among all of the protofilaments within the aggregate and are consequently small. In the analysis of the HbS aggregates in this report we have not attempted to take them into account. Nevertheless, in some cases they may be important. The observation of fibrous aggregates of limited radial extent indicates that the torsional rigidity of the fibers is sufficient to maintain twisting against the torque applied by the stretching of protofilaments on the surface of the aggregate.
15. The twisted crystals have a much larger *p/r* ratio than the other aggregates. Since there is no detailed information on the molecular packing in twisted crystals it is difficult to assess this observation. However, if one assumes that they are made up of double strands interacting side-to-side, there are three possible explanations for the observation: (i) the twisted crystals are not in equilibrium and are still growing radially; the balance of energy between binding energy and energy of stretching is different in the twisted crystals, so that (ii) there is less binding energy available for stretching the double strands; or (iii) the double strands with very long pitch are more rigid and require more energy to stretch. Observations (*4*) suggest that the twisted crystals are metastable intermediates of much larger aggregates and that (i) above is likely to be correct.
16. C. Chothia, A. M. Lesk, G. G. Dodson, D. G. Hodgkin, *Nature (London)* **302**, 500 (1983).
17. C. Chothia and J. Janin, *ibid.* **256**, 705 (1975).
18. D. L. D. Caspar and A. Klug, *Cold Spring Harbor Symp. Quant. Biol.* **27**, 1 (1962).
19. R. H. Crepeau *et al.*, *Proc. Natl. Acad. Sci. U.S.A.* **78**, 1406 (1981).
20. R. J. Vassar, M. J. Potel, R. Josephs, *J. Mol. Biol.* **157**, 395 (1982).
21. R. Josephs, H. S. Jarosch, S. J. Edelstein, *ibid.* **102**, 409 (1976).
22. We thank J. F. Bertles and J. Weisel for helpful discussions. This work is supported by NIH grants GM 29829 and HL 28381.

5 February 1986; accepted 21 October 1986

Petroleum Associated with Polymetallic Sulfide in Sediment from Gorda Ridge

KEITH A. KVENVOLDEN, JOHN B. RAPP, FRANCES D. HOSTETTLER, JANET L. MORTON, J. DAVID KING, GEORGE E. CLAYPOOL

A sediment sample, impregnated with asphaltic petroleum and polymetallic sulfide, was dredged from the southern end of Gorda Ridge (the Escanaba Trough) off northern California, within the offshore Exclusive Economic Zone of the United States. The molecular distributions of hydrocarbons in this petroleum show that it was probably derived from terrestrial organic matter in turbidite sediment filling the Escanaba Trough. Hydrothermal activity at the Gorda Ridge spreading center provided the heat for petroleum formation and was the source of fluids for sulfide mineralization.

GORDA RIDGE IS AN ACTIVE OCEANIC spreading center about 300 km long, bounded on the north and south, respectively, by the Blanco and Mendocino fracture zones (Fig. 1). The southern 90-km end of the ridge, referred to as the Escanaba Trough, is filled with as much as 500 m of Quaternary turbidite sediment (*1*). Within the trough, discrete volcanic centers have uplifted and in some places pierced the trough-filling turbidites (*2*). Siltstone slabs, basaltic glass, and massive polymetallic sulfide (*3*) have been dredged from the flank of one of these volcanic centers at latitude 40°45′N (Fig. 1). One of the samples is unusual in that it is a sediment impregnated with asphaltic petroleum and polymetallic sulfide. The association of petroleum and sulfide is of particular interest, because the sample was recovered within 200 nautical miles (370 km) of the coast of northern California and thus is within the Exclusive Economic Zone of the United States (*4*). The discovery is important with regard to offshore energy and mineral resources.

Evidence for hydrothermal activity at the Escanaba Trough comes from dredge samples obtained in 1983 that contained altered basaltic lava, manganese oxide crusts, nontronite, and sulfide (*5*). After a seismic-reflection survey of the Escanaba Trough in 1985, dredging at station 32 (Fig. 1) recovered 4.5 kg of massive polymetallic sulfide. The sulfide consists mainly of pyrrhotite with minor amounts of sphalerite, chalcopyrite, and galena (*3*); the unoxidized nature of the sulfide minerals indicates that the material was recovered from an actively forming hydrothermal deposit. Similar sulfide deposits have been found around active hot springs on the sediment-covered floor of Guaymas Basin in the Gulf of California (*6*).

Petroleum-like material was first noticed when the sulfide samples were being rinsed with acetone to remove water during the preparation of thin sections; one sample, weighing 185 g, turned the acetone dark brown. An analysis of this sample yielded an organic carbon content of 5.6% by weight, most of which was soluble in methylene chloride. Chromatography and mass spectrometry, both adapted from (*7*), were used to characterize the organic matter. The results of liquid-solid chromatography showed that the extractable organic material in this sample (55 mg/g) is an asphaltic petroleum composed of 2% aliphatic hydrocarbons, 44% aromatic hydrocarbons, and 54% nonhydrocarbons.

The aliphatic and aromatic hydrocarbons were fractionated and identified by gas-liquid chromatography and mass spectrometry (*7*). The following molecular markers were found: (i) a homologous series of *n*-alkanes (*n*-C_{14} to *n*-C_{40}) (Fig. 2A); (ii) isoprenoid hydrocarbons i-16, i-18, i-19 (pristane), and i-20 (phytane) (Fig. 2A); (iii) a series of 17α(H),21β(H) hopanes (C_{27} to C_{35} without C_{28}) including diastereomeric pairs of homohopanes (C_{31} to C_{35}) where 22*R* dominates 22*S* (average 22*S*/22*R* = 0.8) (Fig. 2B); (iv) a series of 17β(H),21α(H) moretanes (C_{29} to C_{31}) (Fig. 2B); (v) steranes (C_{27} to C_{29}) with the 5α(H),14α(H),17α(H)-20*R* isomers more abundant than the 20*S* isomers and low amounts of the 5α(H),14β(H),17β(H)-20*R* and 20*S* diastereomers and rearranged steranes; (vi) a complex mixture of triaromatic steroids (C_{20} and C_{21}) and no monoaromatic steroids (*8*); and (vii) a mixture of polycyclic aromatic hydrocarbons (PAH) containing more nonalkylated than alkylated species (Fig. 2C). No sulfur-containing aromatic hydrocarbons were identified as major components of the aromatic fraction; organic sulfur is probably present, however, in the nonhydrocarbon fraction. All of the hydrocarbons identified are common in petroleum at various levels of maturity (*9*).

The original source of most of the hydrocarbons was probably the organic matter in the Pleistocene and younger turbidites of the Escanaba Trough. These terrigenous sediments, which have organic carbon contents ranging from 0.1 to 0.5% (*10*), derive mostly from the Klamath River and Columbia River drainage basins and were transported across the sea floor to the Escanaba Trough by turbidity currents (*11*). The *n*-alkanes larger than about *n*-C_{24} are characterized by the predominance of odd-carbon-number molecules with a carbon preference

K. A. Kvenvolden, J. B. Rapp, F. D. Hostettler, J. L. Morton, U.S. Geological Survey, Menlo Park, CA 94025.
J. D. King and G. E. Claypool, U.S. Geological Survey, Denver, CO 80225.